Stem Cell Reports
Report
OPEN ACCESS

Debra-Mediated Ci Degradation Controls Tissue Homeostasis in *Drosophila* Adult Midgut

Zhouhua Li,[1,*] Yueqin Guo,[1] Lili Han,[1] Yan Zhang,[1] Lai Shi,[1] Xudong Huang,[2] and Xinhua Lin[1,3,*]
[1]State Key Laboratory of Biomembrane and Membrane Biotechnology, Institute of Zoology, Chinese Academy of Sciences, Beijing 100101, China
[2]School of Optometry and Ophthalmology and Eye Hospital, Wenzhou Medical University, Wenzhou 325000, China
[3]Division of Developmental Biology, Cincinnati Children's Hospital Medical Center, Cincinnati, OH 45229, USA
*Correspondence: zhouhua@ioz.ac.cn (Z.L.), xinhua.lin@ioz.ac.cn or xinhua.lin@cchmc.org (X.L.)
http://dx.doi.org/10.1016/j.stemcr.2013.12.011

SUMMARY

Adult tissue homeostasis is maintained by resident stem cells and their progeny. However, the underlying mechanisms that control tissue homeostasis are not fully understood. Here, we demonstrate that Debra-mediated Ci degradation is important for intestinal stem cell (ISC) proliferation in *Drosophila* adult midgut. Debra inhibition leads to increased ISC activity and tissue homeostasis loss, phenocopying defects observed in aging flies. These defects can be suppressed by depleting Ci, suggesting that increased Hedgehog (Hh) signaling contributes to ISC proliferation and tissue homeostasis loss. Consistently, Hh signaling activation causes the same defects, whereas depletion of Hh signaling suppresses these defects. Furthermore, the Hh ligand from multiple sources is involved in ISC proliferation and tissue homeostasis. Finally, we show that the JNK pathway acts downstream of Hh signaling to regulate ISC proliferation. Together, our results provide insights into the mechanisms of stem cell proliferation and tissue homeostasis control.

INTRODUCTION

Stem cells are critical for tissue homeostasis and regeneration in adult tissues (Simons and Clevers, 2011; Weissman, 2000). The overall decline in tissue regenerative potential with age is accompanied by an age-dependent reduction of adult stem cell functions (Rando, 2006; Rossi et al., 2005; Sharpless and DePinho, 2007). This leads to the hypothesis that stem cell aging may be responsible for age-associated tissue function deterioration and age-related degenerative diseases (Balducci and Ershler, 2005; Bell and Van Zant, 2004; Krtolica, 2005; Van Zant and Liang, 2003). Therefore, understanding the underlying mechanisms that control adult stem cell behavior will provide a platform for therapeutic applications in age-related diseases.

The *Drosophila* adult midgut is an excellent system for studying stem cell biology. Mammalian and fly intestines show marked similarities (Casali and Batlle, 2009; Stainier, 2005; Wang and Hou, 2010). Previous studies demonstrated that fly adult midgut is maintained by ISCs (Micchelli and Perrimon, 2006; Ohlstein and Spradling, 2006). ISCs self-renew and produce enteroblasts (EBs), which will differentiate into either enterocytes (ECs) or enteroendocrine cells (ee) by differential Notch signaling (Micchelli and Perrimon, 2006; Ohlstein and Spradling, 2006; Ohlstein and Spradling, 2007). It has been shown that midgut homeostasis is lost in aged flies, and Jun N-terminal kinase (JNK) signaling contributes to tissue homeostasis loss (Biteau et al., 2008; Choi et al., 2008). However, which endogenous stimuli result in JNK signaling activation in the aging gut and how JNK signaling is regulated remain unexplored.

The Hedgehog (Hh) signaling pathway is evolutionarily conserved in regulating tissue growth and patterning (Ingham et al., 2011; Jiang and Hui, 2008). Aberrant Hh signaling activation causes numerous diseases (Barakat et al., 2010; Taipale and Beachy, 2001). Once released, Hh binds to Patched (Ptc) and alleviates its inhibitory effect on Smoothened (Smo). Smo recruits the Cubitus interruptus (Ci) complex and induces target gene expression (Lum and Beachy, 2004). Ci is polyubiquitinated and degraded in the lysosome, mediated by Debra (Dbr) (Dai et al., 2003). Previous studies have shown that Hh signaling provides a negative feedback signal in regulating the colonic stem cell niche (Büller et al., 2012; Yeung et al., 2011). It was reported that Hh signaling regulates the behavior of ovarian somatic stem cells and hindgut stem cells in fly (Forbes et al., 1996a, 1996b; King et al., 2001; Takashima et al., 2008). However, the function of Hh signaling in adult midgut homeostasis is unclear.

In this study, we provide evidence that Dbr plays an important role in midgut homeostasis. We further demonstrate that JNK signaling acts downstream of Hh signaling in this process. Together, our data uncover an important mechanism that controls ISC proliferation/differentiation and tissue homeostasis.

RESULTS AND DISCUSSION

In order to identify regulators of ISC behavior, we carried out a screen using *esgGal4* in the posterior midgut. From

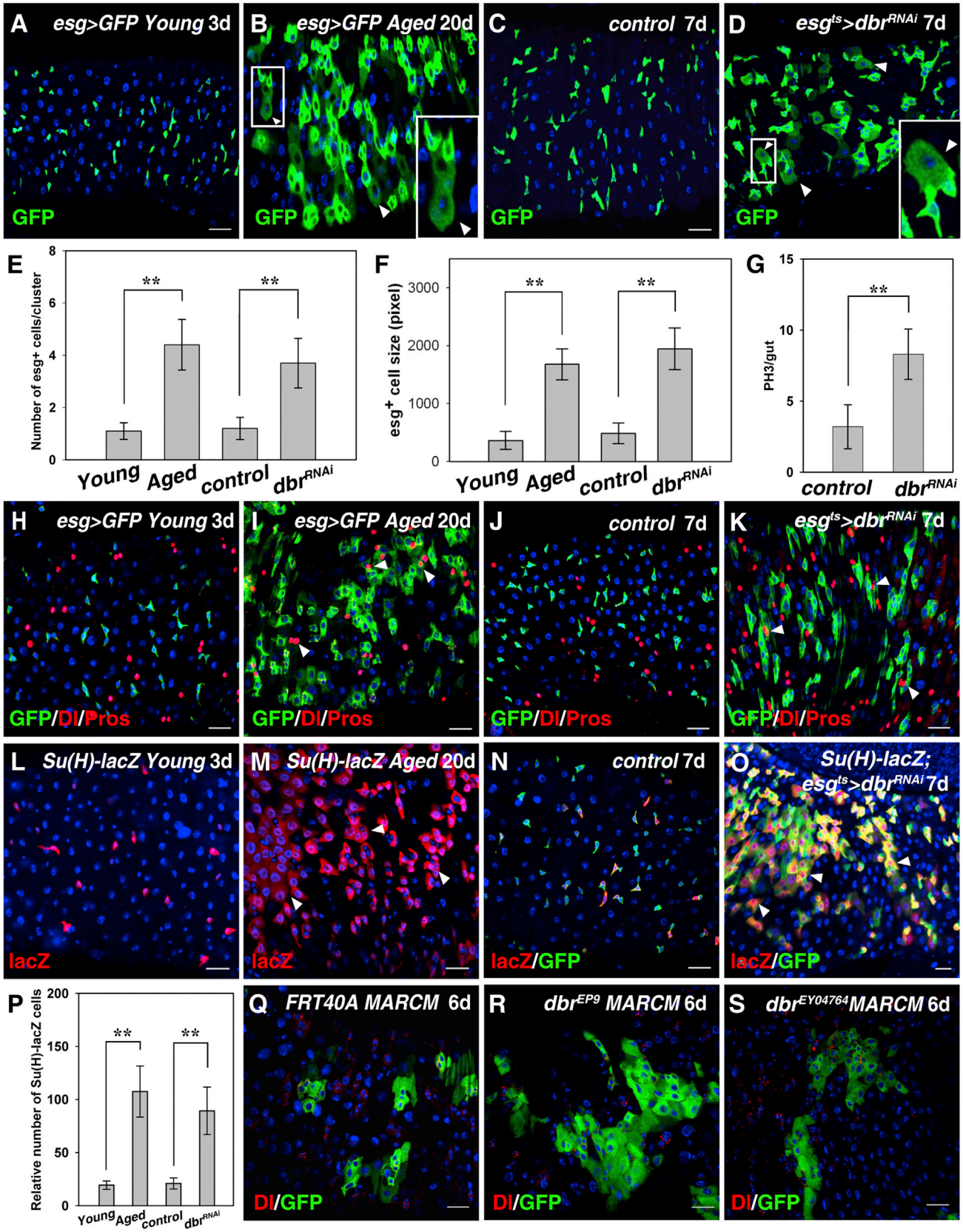

(legend on next page)

this screen, Dbr was identified as a candidate. Single *esg*$^+$ cells are interspersed in young flies (Figure 1A). In aged flies, *esg*$^+$ cells are clustered, enlarged in size, and aberrant in morphology (Figures 1B, 1E, and 1F; Biteau et al., 2008; Choi et al., 2008). Dbr was detected in different intestinal cell types (Figures S1A–S1C available online). When Dbr was depleted (Figure S1D), *esg*$^+$ cells were often clustered, with aberrant morphology (Figures 1C–1E). Their cell size was increased, and many *esg*$^+$ cells were equivalent in size to ECs (Figures 1C, 1D, and 1F). We also observed increased mitosis in these guts (Figure 1G). Because the observed defects were very similar to those observed in aged flies, we speculated that Dbr may be involved in one or more aging-related processes.

In young flies, Dl protein (Delta) could only be detected in individual ISCs or one of two adjacent *esg*$^+$ cells (Figure 1H). In aged flies, high levels of Dl were found in two or more adjacent *esg*$^+$ cells of various sizes (Figure 1I). Moreover, in young flies, ee cells (by Pros) were rarely observed in *esg*$^+$ cells. In aged flies, many Pros$^+$ cells were also *esg*$^+$ (Figures 1H and 1I). In *dbr*-depleted guts, we observed defects similar to those seen in aged flies (Figures 1J and 1K). The differentiation of ISC daughters is regulated by Notch signaling (Micchelli and Perrimon, 2006; Ohlstein and Spradling, 2006, 2007). Notch signaling activation was determined by means of a *Su(H)+GBE-lacZ* reporter (Furriols and Bray, 2001). Notch signaling was activated in EBs in young flies (Figure 1L). In old flies, Notch signaling activation was widespread (Figure 1M). In control flies, Notch signaling was only activated in one of the two adjacent *esg*$^+$ cells (Figure 1N). However, Notch signaling activation could be observed in many cells in *esg*$^+$ clusters (Figures 1O and 1P). To further confirm these defects, we generated *dbr* MARCM clones (Lee and Luo, 2001). Two *dbr* alleles were employed. The size of the ISC clones of both mutants was significantly increased compared with control clones, indicating increased ISC proliferation upon loss of *dbr* (Figures 1Q–1S and 2F). Consistent with the notion that the observed defects in *dbr*-depleted guts resulted from aberrant ISC proliferation/differentiation, these defects could be effectively suppressed by inhibition of epidermal growth factor receptor (EGFR) signaling (Figures S1E–S1H; Jiang et al., 2011). Together, these data demonstrate that Dbr is required for ISC proliferation/differentiation, thereby controlling midgut homeostasis.

We further examined the mechanism(s) underlying Dbr-mediated ISC proliferation. A previous study showed that Dbr can define a Hh-responsive region in the wing disc by ubiquitination and lysosomal degradation of Ci (Dai et al., 2003). We first determined whether Ci is responsible for the defects observed in *dbr* mutants. Indeed, the defects caused by *dbr* knockdown could be suppressed by depletion of *ci* (Figures 1D and 2A–2C). Moreover, inhibition of *ci* alone could effectively inhibit ISC proliferation (Figures S2A–S2C). Furthermore, the size of the ISC clones of both *dbr* mutants was effectively suppressed by codepletion of *ci* (Figures 2D–2F), demonstrating that Ci is the cause of ISC proliferation in the absence of *dbr*.

To further explore the role of Hh signaling in ISC behavior, we generated *ptc* mutant clones. Interestingly, the size of the *ptc*^{S2} ISC clones was significantly increased compared with control clones (Figures 2G–2I). Moreover, in *esg*^{ts} > *ptc*^{RNAi} flies, the number of *esg*$^+$ cells was substantially increased, forming clusters (Figures 2J–2L). These *esg*$^+$ cells were morphologically aberrant, and many *esg*$^+$ cells were increased in cell size (Figures 2J–2L), indicating that tissue homeostasis is lost upon Hh signaling activation. We also observed increased mitosis in *ptc*-depleted guts

Figure 1. Dbr Is Required for Midgut Homeostasis

(A and B) *esg*-positive (*esg*$^+$) cells (green) in young and aged flies. The number of *esg*$^+$ cells is increased; these cells are morphologically aberrant (white arrowheads, boxed inset).

(C) *esg*$^+$ cells (green) in control flies.

(D) *esg*$^+$ cells (green) in *dbr*^{RNAi} flies. GFP signal can be observed in many large cells (white arrowheads, boxed inset).

(E and F) Age-related changes in the guts are quantified by the average of *esg*$^+$ cell number per cluster and the size of *esg*$^+$ cells. Mean ± SEM is shown. n = 3–15 guts. **p < 0.01.

(G) Quantification of midgut PH3$^+$ cells in control and *dbr*^{RNAi}. Mean ± SEM is shown. n = 10–15 guts. **p < 0.01.

(H and I) *esg*$^+$ cells (green) and ISCs (by Dl) in young (H) and aged (I) flies. Pros$^+$ cells (red) are often *esg*$^+$ (white arrowheads).

(J) *esg*$^+$ cells (green) and ISCs (by Dl) in control flies. ee cells labeled by Pros.

(K) The numbers of *esg*$^+$ cells (green) and ISCs (red) are increased in *esg*^{ts} > *dbr*^{RNAi} intestines. Many Pros$^+$ cells (red) are also *esg*$^+$ (white arrowheads).

(L and M) EBs (by *Su(H)-lacZ*) in young (L) and aged (M) flies. Many large cells still retain lacZ staining (white arrowheads, M).

(N) EB (red) in control flies.

(O) The number of EBs (red) in *esg*^{ts} > *dbr*^{RNAi} flies is dramatically increased. Many large cells still retain lacZ staining (white arrowheads).

(P) Quantification of the relative number of EBs in different genotypes as indicated. Mean ± SEM is shown. n = 5–15 guts. **p < 0.01.

(Q) ISC clones in *FRT* control (6D ACI).

(R and S) The *dbr*^{EP9} (R) and *dbr*^{EY04764} (S) ISC MARCM clones are significantly larger than the control clones.

DNA in blue. Scale bars, 20 μm. See also Figure S1.

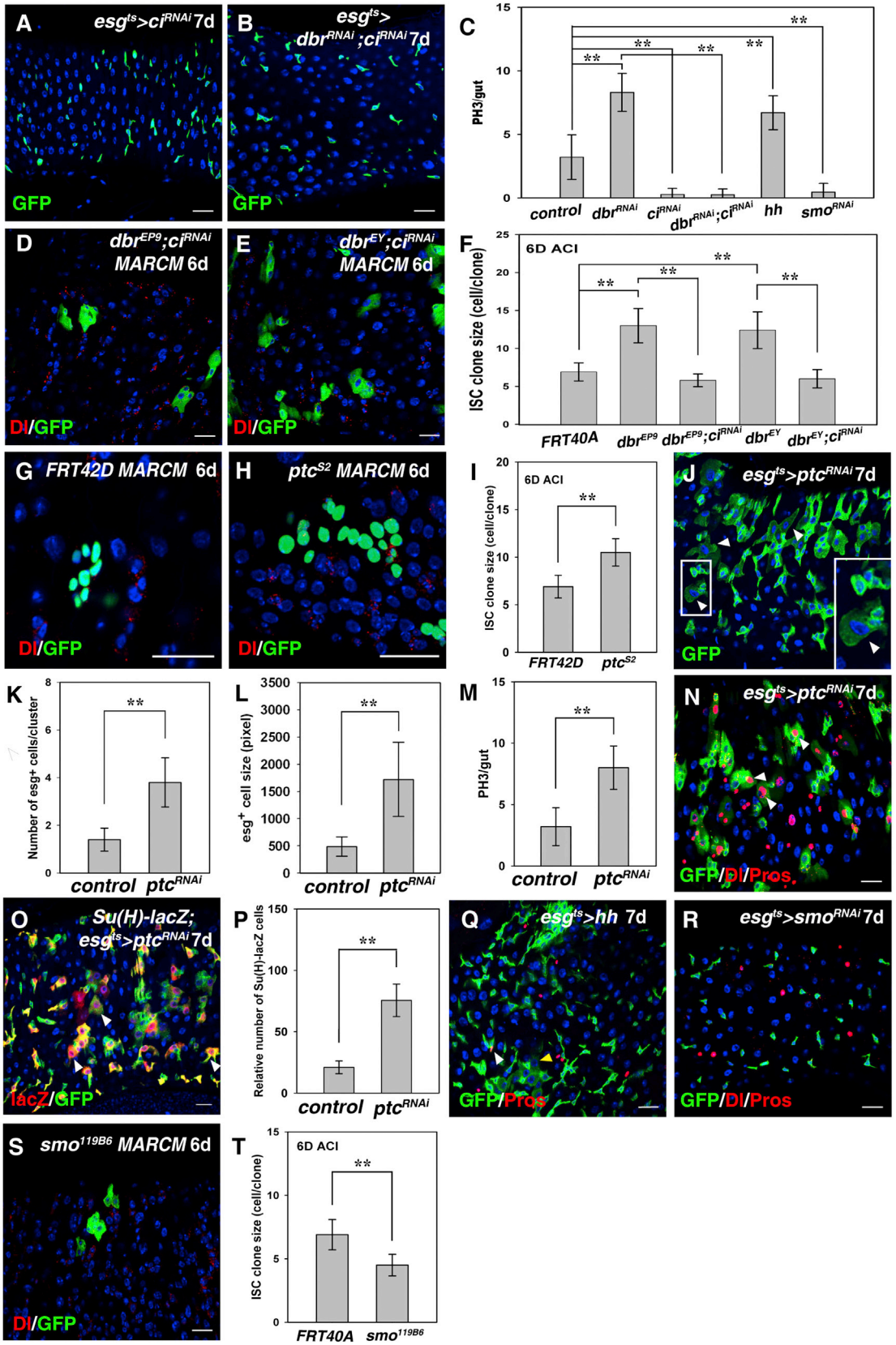

(legend on next page)

(Figure 2M). These phenotypes were very similar to those of aged flies and *dbr* mutants, suggesting that ectopic Hh signaling is responsible for ISC proliferation. Increased Dl was observed in two or more adjacent esg^+ cells of various sizes. Many ee cells were also esg^+ in *ptc*-depleted guts, indicating that homeostasis was lost due to increased ISC proliferation (Figure 2N). Widespread Notch signaling activation was observed in these guts (Figures 2O and 2P), indicating that aberrant progeny differentiation occurred. Lastly, ISC proliferation was increased upon ectopic Hh expression. These esg^+ cells were aberrant in morphology. Meanwhile, some $Pros^+$, esg^+ cells were produced (Figures 2C and 2Q). Collectively, these data demonstrate that ectopic Hh signaling could result in ISC proliferation and misdifferentiation, leading to midgut homeostasis loss. Consistently, ISC proliferation was inhibited in $esg^{ts} > smo^{RNAi}$ flies (Figures 2C and 2R). Similarly, the size of the *smo* ISC clones was significantly reduced (Figures 2S and 2T). Furthermore, we found that midgut regeneration under stress conditions was compromised by inhibition of Hh signaling (Figures S2D–S2G).

The aforementioned experiments demonstrated the essential roles of Dbr/Hh signaling in midgut homeostasis. Next, we examined the source(s) of Hh involved in this process. We determined *hh* expression by using an *hh-lacZ* enhancer and Hh antibody. A high level of Hh expression was found in the anterior adult hindgut (Figures 3A and 3B; Takashima et al., 2008). In the posterior midgut, Hh expression was detected in the visceral muscles (VMs) and various intestinal cells (Figures 3C–3H). Moreover, we found that Hh expression was significantly increased in aged and stressed flies (Figure S3A; Buchon et al., 2009). Next, we discriminated the source of functional Hh proteins via RNAi and various Gal4 drivers. However, ISC proliferation could still be observed after induction of hh^{RNAi} (Figures 3I–3L; data not shown), indicating that Hh proteins from different sources play a redundant role in ISC proliferation. Consistently, Hh protein could be detected in the VMs and intestinal cells when ectopic *hh* expression was induced in the trachea and VMs, respectively (Figure S3B). These data indicate that Hh protein can be transported to the midgut epithelium from its various producing sources, consistent with our recent finding that Dpp (Decapentaplegic) can be transported from the trachea to the midgut epithelium (Li et al., 2013). Consistently, ISC proliferation was effectively suppressed in $tub^{ts} > hh^{RNAi}$ flies and hh^{ts} mutants (Figures 3L–3Q). Together, these data demonstrate that Hh from multiple sources is involved in midgut homeostasis.

How does Hh signaling regulate midgut homeostasis? Damage by oxidative stress is one cause of age-related homeostasis loss. Previous studies have shown that JNK signaling increases cellular stress tolerance and contributes to tissue homeostasis loss in old and stressed guts (Biteau et al., 2008; Oh et al., 2005; Wang et al., 2003, 2005). Therefore, it is possible that Hh signaling may result in JNK signaling activation, causing midgut homeostasis loss. Indeed, we found that JNK signaling was dramatically elevated in aged flies (Figures 4A–4C). Moreover, Hh signaling activated by depletion of *dbr* or *ptc* substantially increased JNK signaling levels (Figures 4C–4F). Furthermore, JNK signaling activation in aged flies was greatly suppressed in $esg^{ts} > ci^{RNAi}$ flies (Figures 4B and 4G). Importantly, midgut homeostasis loss caused by *dbr* knockdown

Figure 2. Dbr-Mediated Ci Degradation Controls Tissue Homeostasis

(A) esg^+ cells (green) in $esg^{ts} > ci^{RNAi}$ flies.
(B) The accumulation of esg^+ cells in $esg^{ts} > dbr^{RNAi}$ flies is effectively suppressed by coinhibition of Ci.
(C) Quantification of midgut $PH3^+$ cells in different genotypes as indicated. Mean ± SEM is shown. n = 10–15 guts. **p < 0.01.
(D and E) The large ISC MARCM clones observed in dbr^{EP9} (D) and $dbr^{EY04764}$ (E) are effectively suppressed by simultaneous Ci depletion.
(F) Quantification of ISC clone size in different genotypes as indicated. Mean ± SEM is shown. n = 5–15 guts. **p < 0.01.
(G and H) The ptc^{S2} ISC MARCM clones (H) are larger than the control clones (G).
(I) Quantification of ISC clone size in control and ptc^{S2}. Mean ± SEM is shown. n = 5–15 guts. **p < 0.01.
(J) Midgut homeostasis is lost in ptc^{RNAi} flies (white arrowheads, boxed inset).
(K and L) Quantification of esg^+ cells per cluster (K) and the area of esg^+ cells (L) in control and ptc^{RNAi} intestines. Mean ± SEM is shown. n = 5–15 guts. **p < 0.01.
(M) Quantification of midgut PH3+ cells in control and ptc^{RNAi}. Mean ± SEM is shown. n = 10–15 guts. **p < 0.01.
(N) The number of esg^+ cells (green) and ISCs (red) is increased in $esg^{ts} > ptc^{RNAi}$ flies. Many $Pros^+$ cells are also esg^+ (white arrowheads).
(O) The number of EBs (red) in $esg^{ts} > ptc^{RNAi}$ flies is dramatically increased. Many large cells still retain lacZ staining (white arrowheads).
(P) Quantification of the relative number of EBs in control and ptc^{RNAi} intestines. Mean ± SEM is shown. n = 5–15 guts. **p < 0.01.
(Q) The number of esg^+ cells is increased in $esg^{ts} > hh$ intestines. The size of some esg^+ cells is increased (yellow arrowhead), and some $Pros^+$ cells are also esg^+ (white arrowhead).
(R) esg^+ cells (green) and ISCs (red) in $esg^{ts} > smo^{RNAi}$ flies; ee cells in red.
(S) The smo^{119B6} ISC MARCM clones are smaller than the control clones.
(T) Quantification of ISC clone size in control and smo^{119B6}. Mean ± SEM is shown. n = 5–15 guts. **p < 0.01.
DNA in blue. Scale bars, 20 μm. See also Figure S2.

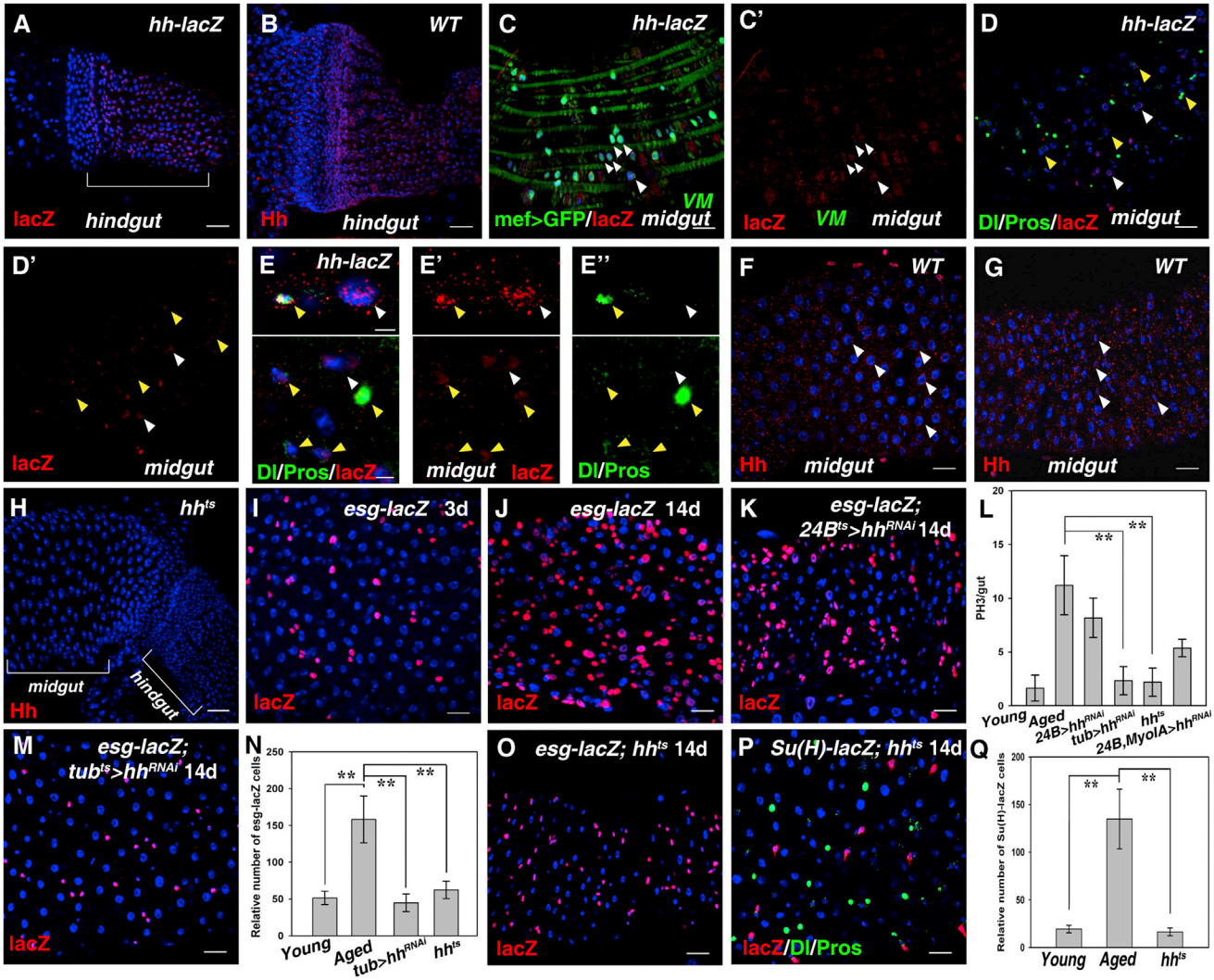

Figure 3. Hh Protein Originates from Multiple Sources

(A) Hh (by *hh-lacZ*) is expressed in adult hindgut (white bracket).
(B) Hh (by Hh antibody) can be detected in adult hindgut.
(C and C') Hh (by *hh-lacZ*) is expressed in VMs (green) (white arrowheads).
(D and E) Hh (by *hh-lacZ*) is expressed in large and small cells (Dl, Pros in green) in adult midgut (white and yellow arrowheads).
(F–H) Hh (by Hh antibody) can be detected in large and small cells in adult midgut (white arrowheads). No such signals can be detected in hh^{ts} (H).
(I and J) esg^+ cells (red) in 3-day-old (I) and 14-day-old (J) *esg-lacZ* flies at 29°C.
(K) Age-related accumulation of esg^+ cells could not be suppressed in $24B^{ts} > hh^{RNAi}$ flies.
(L) Quantification of midgut PH3+ cells in different genotypes as indicated. Mean ± SEM is shown. n = 10–15 guts. **p < 0.01.
(M) Age-related accumulation of esg^+ cells (red) could be effectively suppressed in $tub^{ts} > hh^{RNAi}$ flies.
(N) Quantification of the relative number of esg^+ cells in different genotypes as indicated. Mean ± SEM is shown. n = 5–10 guts. **p < 0.01.
(O) Age-related accumulation of esg^+ cells (red) could be effectively suppressed in hh^{ts} (hh^{AC}/hh^{ts}) flies.
(P) Age-related accumulation of ISCs (Dl in red) and EBs (lacZ in green) could be effectively suppressed in hh^{ts} flies.
(Q) Quantification of the relative number of EBs in the indicated flies. Mean ± SEM is shown. n = 5–10 guts. **p < 0.01.
DNA in blue. Scale bars, 20 μm except (E) (5 μm). See also Figure S3.

was effectively suppressed by coinhibition of JNK signaling (Figures 4H–4O). These data argue that JNK signaling acts downstream of Hh signaling, contributing to tissue homeostasis loss. On the basis of our observations, we propose that Hh from multiple sources induces Hh signaling in ISCs to promote ISC proliferation/differentiation, causing

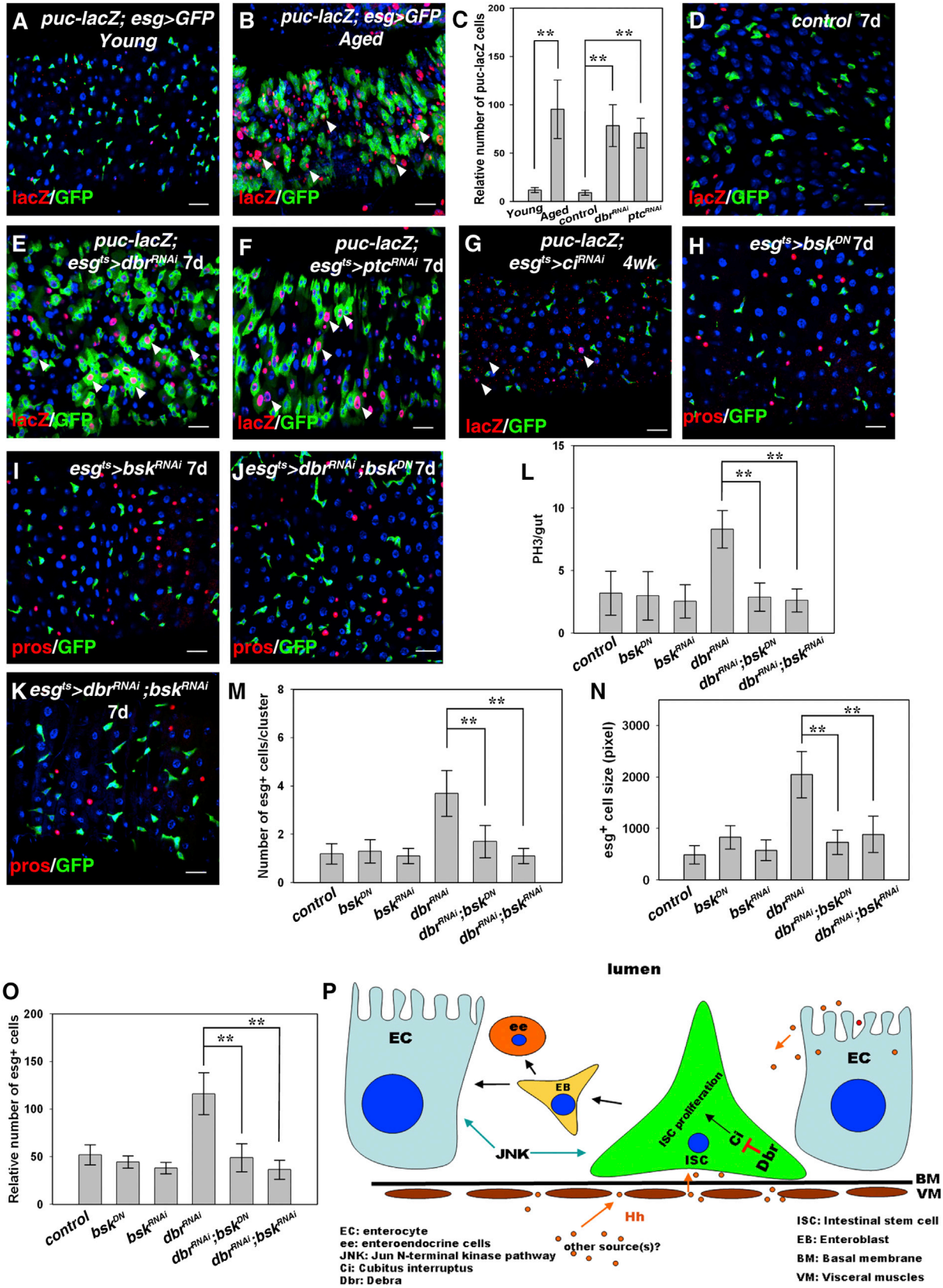

(legend on next page)

tissue homeostasis loss. This detrimental effect of Hh signaling is safeguarded by Dbr, which maintains a proper level of Hh signaling in ISCs (Figure 4P). Our data suggest that JNK signaling acts downstream of Hh signaling in controlling tissue homeostasis.

Our data demonstrate the essential role of Dbr in controlling tissue homeostasis. Stem cells are influenced by both intrinsic and extrinsic factors (Casali and Batlle, 2009; Radtke and Clevers, 2005; Xie and Spradling, 2000). Previous studies have demonstrated that fly ISCs receive various extrinsic signals from VMs and the midgut epithelium itself (Jiang et al., 2009, 2011; Lin et al., 2008). Our recent data also demonstrated that BMP from tracheal cells is an extrinsic signal required for midgut hemostasis (Li et al., 2013). The present study highlights Hh as another extrinsic signal that is essential for ISC physiology. Up to now, however, the intrinsic factors that control ISC behaviors have not been well studied. Here, we identified Dbr as an intrinsic factor. Proper control of the regenerative and self-renewal capacity of stem cells in the intestinal epithelium is of particular importance for long-lived organisms. Failure of this regulation in older individuals is reflected by the high incidence of intestinal adenomatous polyps (Radtke and Clevers, 2005). It has been reported that Shh levels are elevated in human gastric adenomas and intestinal metaplasias, suggesting that Hh overactivation may be involved in early gastric carcinomas (Parkin and Ingham, 2008). We found that the expression of Hh pathway components is increased in aging guts (Figure S4). Furthermore, although *dbr* expression increases as flies age, increased Hh signaling together with the activation of other signaling pathways, such as JAK/Stat and p38, may overcome the inhibitory effect of Dbr in aging flies, leading to midgut homeostasis loss (Figures S1A–S1C and S4).

JNK signaling promotes the expression of cytoprotective genes in flies, which contributes to tissue homeostasis loss in aged guts (Biteau et al., 2008). We found that JNK activity was increased in *dbr*- and *ptc*-depleted guts, and further inhibition of JNK activity in these guts effectively suppressed these defects. Importantly, JNK signaling activation was greatly suppressed by inhibition of Ci (Figures 4B–4G). These data indicate that JNK signaling acts downstream of Hh signaling in tissue homeostasis control (Figures 4C–4O). Interestingly, the guts of senescent mice contain increased numbers of clonogenic cells, reminiscent of the age-related changes in flies (Martin et al., 1998). Based on the evolutionary conservation of JNK signaling (Weston and Davis, 2007), it is expected that its effects on midgut homeostasis are also conserved. Further studies are needed to determine which stimuli result in JNK activation in *dbr*- and *ptc*-depleted guts. Oxidative stress is a plausible inducer. Additionally, other stimuli, such as enteric infection, can also activate JNK. Further analysis will provide new insight into the mechanisms of tissue homeostasis control.

EXPERIMENTAL PROCEDURES

Fly Lines and Husbandry

Flies were maintained on standard media at 25°C. Crosses were raised in 18°C incubators. Information regarding the alleles and transgenes used in this study can be found in FlyBase (http://flybase.org) and Supplemental Experimental Procedures.

Immunostaining and Fluorescence Microscopy

Immunostaining of intestines was performed as previously described (Li et al., 2013). The primary antibodies used were mouse mAb anti-Dl (C594.9B, 1:50) and mouse mAb anti-Pros (MR1A, 1:100; both obtained from DSHB), rabbit anti-β-galactosidase

Figure 4. JNK Signaling Acts Downstream of Hh Signaling to Control Midgut Homeostasis

(A) JNK signaling activation (by *puc-lacZ*) in young flies.

(B) JNK signaling is dramatically activated (by *puc-lacZ*, white arrowheads) in aged flies.

(C) Quantification of the relative number of *puc-lacZ* cells in different genotypes as indicated. Mean ± SEM is shown. n = 5–15 guts. **p < 0.01.

(D) JNK signaling activation (by *puc-lacZ*) in control flies.

(E and F) JNK signaling is dramatically activated in $esg^{ts} > dbr^{RNAi}$ (E) and (F) $esg^{ts} > ptc^{RNAi}$ flies (white arrowheads).

(G) Dramatic JNK signaling activation is not observed in $esg^{ts} > ci^{RNAi}$ flies (4 weeks, white arrowheads).

(H and I) esg^{+} cells (green) in $esg^{ts} > bsk^{DN}$ (H) and $esg^{ts} > bsk^{RNAi}$ (I) flies; ee cells are labeled by Pros (red).

(J and K) The accumulation of esg^{+} cells resulting from dbr^{RNAi} is effectively suppressed by coexpression of bsk^{DN} (J) and bsk^{RNAi} (K).

(L) Quantification of midgut $PH3^{+}$ cells in different genotypes as indicated. Mean ± SEM is shown. n = 10–15 guts. **p < 0.01.

(M–O) Quantification of the number of esg^{+} cells per cluster (M), the area of esg^{+} cells (N), and the relative number of esg^{+} cells (O) in different genotypes as indicated. Mean ± SEM is shown. n = 5–15 guts. **p < 0.01.

(P) Proposed model for the role of Dbr-mediated Ci degradation in controlling midgut homeostasis. Hh protein is produced from multiple sources (midgut, VMs, hindgut, and possibly other unidentified tissues). The level of Hh signaling in ISCs is modulated by Dbr, thereby maintaining ISCs at a proper proliferation/differentiation rate to prevent them from proliferating excessively. JNK signaling acts downstream of Hh signaling. BM, basal membrane.

DNA in blue. Scale bars, 20 μm. See also Figure S4.

(1:5,000; Cappel), mouse anti-β-galactosidase (1:1,000; Cell Signaling), rabbit anti-pH3 (1:2,000; Millipore), rabbit anti-Dbr (1:100; a gift from Dr. S. Ishii), and rabbit anti-RFP (1:200; Abcam). All images were captured by a Zeiss LSM780 inverted confocal microscope and processed in Adobe Photoshop and Illustrator.

MARCM ISC Mosaic Analysis

The ISC clones were induced by heat shocking 3- to 5-day-old adult flies at 37°C for 1 hr. The flies were maintained at 25°C and transferred to new vials every day. The sizes of the marked clones were assayed at 6 days after clone induction (6D ACI).

Data analysis

PH3 numbers were scored under Zeiss Z2/LSM780 microscopes. The number scored is indicated in the text. The number of esg^+ cells per cluster was determined in at least five guts. Quantification of the cell size of esg^+ cells was performed using Adobe Photoshop. The size of at least 20 cells in three different guts was determined for each condition. The relative number of esg^+ cells and EBs was determined using Image-Pro Plus from confocal images. Student's t test was used for statistical analysis; $^*p < 0.05$ was considered significant and data are presented as mean ± SEM. Sigma plot software was used for graph generation. The graphs were further modified using Adobe Photoshop and Illustrator.

SUPPLEMENTAL INFORMATION

Supplemental Information includes Supplemental Experimental Procedures and four figures and can be found with this article online at http://dx.doi.org/10.1016/j.stemcr.2013.12.011.

ACKNOWLEDGMENTS

We thank N. Perrimon, S. Bray, S. Hou, and S. Ishii for reagents; the Bloomington Stock Center, Vienna *Drosophila* RNAi Center, NIG-FLY Center, and TRiP at Harvard Medical School for fly stocks; and DSHB for antibodies. We gratefully acknowledge comments by Dr. T.Y. Belenkaya, L. Ray, and J. You. We apologize to the colleagues whose work could not be cited because of space restrictions. This work was supported by grants from the National Natural Science Foundation of China (31271582 and 31030049), Strategic Priority Research Program of the Chinese Academy of Sciences grant XDA01010101, and the National Basic Research Program of China (2011CB943901 and 2011 CB943902). We declare no conflicts of interest.

Received: April 17, 2013
Revised: December 18, 2013
Accepted: December 19, 2013
Published: January 30, 2014

REFERENCES

Büller, N.V.J.A., Rosekrans, S.L., Westerlund, J., and van den Brink, G.R. (2012). Hedgehog signaling and maintenance of homeostasis in the intestinal epithelium. Physiology (Bethesda) *27*, 148–155.

Balducci, L., and Ershler, W.B. (2005). Cancer and ageing: a nexus at several levels. Nat. Rev. Cancer *5*, 655–662.

Barakat, M.T., Humke, E.W., and Scott, M.P. (2010). Learning from Jekyll to control Hyde: Hedgehog signaling in development and cancer. Trends Mol. Med. *16*, 337–348.

Bell, D.R., and Van Zant, G. (2004). Stem cells, aging, and cancer: inevitabilities and outcomes. Oncogene *23*, 7290–7296.

Biteau, B., Hochmuth, C.E., and Jasper, H. (2008). JNK activity in somatic stem cells causes loss of tissue homeostasis in the aging Drosophila gut. Cell Stem Cell *3*, 442–455.

Buchon, N., Broderick, N.A., Poidevin, M., Pradervand, S., and Lemaitre, B. (2009). Drosophila intestinal response to bacterial infection: activation of host defense and stem cell proliferation. Cell Host Microbe *5*, 200–211.

Casali, A., and Batlle, E. (2009). Intestinal stem cells in mammals and Drosophila. Cell Stem Cell *4*, 124–127.

Choi, N.H., Kim, J.G., Yang, D.J., Kim, Y.S., and Yoo, M.A. (2008). Age-related changes in Drosophila midgut are associated with PVF2, a PDGF/VEGF-like growth factor. Aging Cell *7*, 318–334.

Dai, P., Akimaru, H., and Ishii, S. (2003). A hedgehog-responsive region in the Drosophila wing disc is defined by debra-mediated ubiquitination and lysosomal degradation of Ci. Dev. Cell *4*, 917–928.

Forbes, A.J., Lin, H., Ingham, P.W., and Spradling, A.C. (1996a). hedgehog is required for the proliferation and specification of ovarian somatic cells prior to egg chamber formation in Drosophila. Development *122*, 1125–1135.

Forbes, A.J., Spradling, A.C., Ingham, P.W., and Lin, H. (1996b). The role of segment polarity genes during early oogenesis in Drosophila. Development *122*, 3283–3294.

Furriols, M., and Bray, S. (2001). A model Notch response element detects Suppressor of Hairless-dependent molecular switch. Current biology: CB *11*, 60–64.

Ingham, P.W., Nakano, Y., and Seger, C. (2011). Mechanisms and functions of Hedgehog signalling across the metazoa. Nat. Rev. Genet. *12*, 393–406.

Jiang, J., and Hui, C.C. (2008). Hedgehog signaling in development and cancer. Dev. Cell *15*, 801–812.

Jiang, H., Patel, P.H., Kohlmaier, A., Grenley, M.O., McEwen, D.G., and Edgar, B.A. (2009). Cytokine/Jak/Stat signaling mediates regeneration and homeostasis in the Drosophila midgut. Cell *137*, 1343–1355.

Jiang, H., Grenley, M.O., Bravo, M.-J., Blumhagen, R.Z., and Edgar, B.A. (2011). EGFR/Ras/MAPK signaling mediates adult midgut epithelial homeostasis and regeneration in Drosophila. Cell Stem Cell *8*, 84–95.

King, F.J., Szakmary, A., Cox, D.N., and Lin, H. (2001). Yb modulates the divisions of both germline and somatic stem cells through piwi- and hh-mediated mechanisms in the Drosophila ovary. Mol. Cell *7*, 497–508.

Krtolica, A. (2005). Stem cell: balancing aging and cancer. Int. J. Biochem. Cell Biol. *37*, 935–941.

Lee, T., and Luo, L. (2001). Mosaic analysis with a repressible cell marker (MARCM) for Drosophila neural development. Trends Neurosci. *24*, 251–254.

Li, Z., Zhang, Y., Han, L., Shi, L., and Lin, X. (2013). Trachea-derived Dpp controls adult midgut homeostasis in Drosophila. Dev. Cell *24*, 133–143.

Lin, G., Xu, N., and Xi, R. (2008). Paracrine Wingless signalling controls self-renewal of Drosophila intestinal stem cells. Nature *455*, 1119–1123.

Lum, L., and Beachy, P.A. (2004). The Hedgehog response network: sensors, switches, and routers. Science *304*, 1755–1759.

Martin, K., Potten, C.S., Roberts, S.A., and Kirkwood, T.B. (1998). Altered stem cell regeneration in irradiated intestinal crypts of senescent mice. J. Cell Sci. *111*, 2297–2303.

Micchelli, C.A., and Perrimon, N. (2006). Evidence that stem cells reside in the adult Drosophila midgut epithelium. Nature *439*, 475–479.

Oh, S.W., Mukhopadhyay, A., Svrzikapa, N., Jiang, F., Davis, R.J., and Tissenbaum, H.A. (2005). JNK regulates lifespan in Caenorhabditis elegans by modulating nuclear translocation of forkhead transcription factor/DAF-16. Proc. Natl. Acad. Sci. USA *102*, 4494–4499.

Ohlstein, B., and Spradling, A. (2006). The adult Drosophila posterior midgut is maintained by pluripotent stem cells. Nature *439*, 470–474.

Ohlstein, B., and Spradling, A. (2007). Multipotent Drosophila intestinal stem cells specify daughter cell fates by differential notch signaling. Science *315*, 988–992.

Parkin, C.A., and Ingham, P.W. (2008). The adventures of Sonic Hedgehog in development and repair. I. Hedgehog signaling in gastrointestinal development and disease. Am. J. Physiol. Gastrointest. Liver Physiol. *294*, G363–G367.

Radtke, F., and Clevers, H. (2005). Self-renewal and cancer of the gut: two sides of a coin. Science *307*, 1904–1909.

Rando, T.A. (2006). Stem cells, ageing and the quest for immortality. Nature *441*, 1080–1086.

Rossi, D.J., Bryder, D., Zahn, J.M., Ahlenius, H., Sonu, R., Wagers, A.J., and Weissman, I.L. (2005). Cell intrinsic alterations underlie hematopoietic stem cell aging. Proc. Natl. Acad. Sci. USA *102*, 9194–9199.

Sharpless, N.E., and DePinho, R.A. (2007). How stem cells age and why this makes us grow old. Nat. Rev. Mol. Cell Biol. *8*, 703–713.

Simons, B.D., and Clevers, H. (2011). Strategies for homeostatic stem cell self-renewal in adult tissues. Cell *145*, 851–862.

Stainier, D.Y. (2005). No organ left behind: tales of gut development and evolution. Science *307*, 1902–1904.

Taipale, J., and Beachy, P.A. (2001). The Hedgehog and Wnt signalling pathways in cancer. Nature *411*, 349–354.

Takashima, S., Mkrtchyan, M., Younossi-Hartenstein, A., Merriam, J.R., and Hartenstein, V. (2008). The behaviour of Drosophila adult hindgut stem cells is controlled by Wnt and Hh signalling. Nature *454*, 651–655.

Van Zant, G., and Liang, Y. (2003). The role of stem cells in aging. Exp. Hematol. *31*, 659–672.

Wang, P., and Hou, S.X. (2010). Regulation of intestinal stem cells in mammals and Drosophila. J. Cell. Physiol. *222*, 33–37.

Wang, M.C., Bohmann, D., and Jasper, H. (2003). JNK signaling confers tolerance to oxidative stress and extends lifespan in Drosophila. Dev. Cell *5*, 811–816.

Wang, M.C., Bohmann, D., and Jasper, H. (2005). JNK extends life span and limits growth by antagonizing cellular and organism-wide responses to insulin signaling. Cell *121*, 115–125.

Weissman, I.L. (2000). Stem cells: units of development, units of regeneration, and units in evolution. Cell *100*, 157–168.

Weston, C.R., and Davis, R.J. (2007). The JNK signal transduction pathway. Curr. Opin. Cell Biol. *19*, 142–149.

Xie, T., and Spradling, A.C. (2000). A niche maintaining germ line stem cells in the Drosophila ovary. Science *290*, 328–330.

Yeung, T.M., Chia, L.A., Kosinski, C.M., and Kuo, C.J. (2011). Regulation of self-renewal and differentiation by the intestinal stem cell niche. Cell. Mol. Life Sci. *68*, 2513–2523.